On the Properties and Processing of Polyethylene Terephthalate/Styrene-Butadiene Rubber Blend

A. SÁNCHEZ-SOLÍS,* M. R. ESTRADA, J. CRUZ,** *and* O. MANERO

Instituto de Investigaciones en Materiales, UNAM
A. P. 70-360, México, D. F. 04510

***Facultad de Química, UNAM*

The mixing of incompatible polymers such as polyethylene terephthalate (PET) and styrene-butadiene rubber (SBR) produces a blend with poor mechanical and impact properties, because polymeric phases interact weakly with each other and segregate. The use of SBR grafted with maleic anhydride (MAH) increases the compatibility of the SBR-PET system by generating higher interactions and chemical links between the ingredients of the blend. The induced compatibility is reflected in the 2.5-fold increase in the impact resistance of the blend as compared to that of pure PET. The grafting reaction to produce SBR-g-MAH is carried out by reactive extrusion using a reaction initiator, benzoyl peroxide (BPO), and the extent of the reaction depends on the concentration of MAH and BPO. Results indicate the close relationship between processing conditions and microstructural parameters, such as particle diameter and interparticle distances of the dispersed rubber phase, necessary to achieve the optimum impact resistance.

INTRODUCTION

Engineering plastics have become a massive market for specific applications in many industries. Some of the most popular are polyethylene terephthalate (PET), acrylonitrile butadiene styrene (ABS), polycarbonate (PC), polysulfone (PSf), and polyimides (PI), among others (1). Blends of these polymers have been elaborated to obtain materials with required physical and chemical properties. Ample commercial and scientific interests exist to combine the different characteristics of various polymers to improve faulty properties of a particular material. Examples of these systems are: ABS-PVC (2), nylon-rubber (3), nylon-EPDM-MAH (4), natural rubber-polyolefins-MAH (5), thermoplastic elastomers (TPE)-LLDPE (6), polystyrene-EPDM (7), PBT-EPM (8), PPO-PS-EPDM (9), PP-EPDM (10) and PBT-maleated EPDM (11). For the specific case of PET we can also mention blends of PET-nylon 6,6 (12–17), PET-PP (18, 19), PET-polyolefins (20, 21), PET-cellulose (22), PET-EMMA (23), PET-methylpolyacrilate (24), PET-bisphenol A (25), PET-ethylene methacrylic acid (26), and PET-PBT (27). It is well known that most of these blends are immiscible and present inferior physical properties than their components by lack of interaction among the polymer phases, which causes premature flaws of the material. It is also well known that the addition of reactive groups on the polymer chain through grafting induces reactions at the interface of the polymer phases, generating chemical links and increasing the compatibility of the blend.

In this study in particular, SBR grafted with maleic anhydride (SBRg) is used to improve the compatibility of the PET-SBR blend. The grafting reaction is carried out by reactive extrusion via free radicals, using benzoyl peroxide as reaction initiator.

EXPERIMENTAL

Materials

PET from Celanese (Mexico) had a density of 1.425 g/cm^3 according to ASTM D792. Differential scanning calorimetry (DSC) was used to determine the melting point at 249°C (with a heating speed of 10°C/min under nitrogen atmosphere), a crystallinity of 37% (28, 29) and also a glass transition at 74°C. An average molecular weight of 26,000 g/mol was determined by high temperature GPC using m-cresol. An intrinsic viscosity of 0.850 dl/g (30) was measured with an Ubbelhode viscometer. Styrene-butadiene rubber (SBR) from Negromex (Solprene 416) had a density of 0.919 g/cm^3 (according to ASTM D792). The styrene block content was 30% (31). An average molecular

*To whom correspondence should be addressed.

weight of 105,500 was determined by high temperature GPC using 1,2,4 trichlorobenzene. The glass transition temperature (–89°C) was determined by DSC with a heating speed of 10°C/min under nitrogen atmosphere. The maleic anhydride (MAH) was recrystallized twice and benzoyl peroxide (BPO) was used as received. The maleic anhydride was recrystallized using chloroform at 53–54°C (which was previously dried with P_2O_5) under stirring with reflux. The resulting solution was vacuum-filtered and the soluble portion was cooled up to precipitation. The precipitated material was dried under vacuum obtaining crystals of maleic anhydride. The additives to prevent oxidation were Irganox 1076 for the rubber and Irganox 1010 for PET, from Ciba-Geigy.

Equipment

A Haake Rheocord 90 TW100 twin-screw conical counter-rotating extruder with length of 331 mm, was used in the reactive extrusion work. Samples were dried in a Pagani dehumidifier provided with molecular meshes. The specimens for impact and traction tests were produced in a Demag Ergotech 50 injection-molding machine. An Instron tester model 1125 was used for traction tests following ASTM D638. Impact tests were carried out under ASTM D256-92-type Izod-notched. Micrographs for particle diameter and interparticular distances were taken in a Jeol JSM-70 transmission electron microscope equipped with a Leica Quantimet 500 image analyzer.

PROCEDURE

Grafting of SBR

SBR previously dried at 80°C is mixed with benzoyl peroxide (BPO) and maleic anhydride (MAH). The grafting reaction is carried out by reactive extrusion at 160°C using three screw speeds: 30, 70 and 100 rpm. The reacted amount of MAH is determined by measuring the acid number by the following procedure: One gram of grafted rubber is dissolved into 100 ml toluene with a reflux at 65°C for three hours. 50 ml of water are added and the solution separates into three phases: organic, gel and aqueous phases. An aliquot of the organic phase is taken and titrated with a KOH-ethanol solution (0.1 N) using thymol blue as indicator. A KOH excess of 0.5 ml is added to the solution (we observe a color change to blue), and subsequently, this solution is retitrated with HCl up to 0.05 N (color changes to yellow). The acid number and the MAH reacted percentage are calculated according to:

$$N^{o}\ acid\ (mg\ KOH/g\ rubber) = ml\ KOH * N\ KOH * 56.1/1\ g\ rubber \quad (1)$$

$$\%\ MAH\ that\ reacts = (N^{o}acid * 98/2*561)\ (g\ of\ rubber/g\ of\ MAH) \quad (2)$$

Reaction starts by free radicals as BPO is added (32-33). Without BPO, the reaction still proceeds because of the thermomechanical stresses produced in the extrusion process (34). According to the literature, small quantities of peroxide are normally used (approximately 0.06% of the rubber weight) (33, 35, 36).

Preparation of the PET-SBRg Blends

PET and SBRg are dried during 6 hours at 110°C and 80°C, respectively. The blends are processed by extrusion at 50 rpm with a temperature profile of 245–260°C. Specimens for impact and tension tests are injection-molded with a mold temperature of 7°C, injection speed of 85 mm/s, screw speed of 200 rpm and with a feed-stage temperature of 260°C. The mold temperature was kept low to approach a quenching operation where the mold is sufficiently cold and the cooling time in the mold is short. Under these conditions it is possible to obtain a mostly amorphous material. Similar conditions have been considered elsewhere (37, 38). Tension tests are carried out at a strain rate of 50 mm/min according to ASTM D638. Impact Izod specimens are notched (2 mm in depth) with an angle of 45°. Samples of 1.5 mm in thickness are cut from the fracture surfaces and gold-coated for the scanning electron microscopy studies.

RESULTS AND DISCUSSION

Primarily, it is necessary to evaluate the extent of the grafting reaction MAH-SBR as a function of the amount of MAH added initially to the rubber. The amount of peroxide used is fixed initially to 3 wt% with respect to the amount of MAH added. Upon dissolving the resulting SBR in toluene following the procedure outlined previously, three phases are produced: the gel phase contains the crosslinked material, the organic phase contains the MAH-grafted material and the aqueous phase contains the non-reacted anhydride. As observed in *Fig. 1*, the percentage of MAH that remains in each phase is shown as a function of the MAH amount added initially. The MAH concentration in the organic phase presents a maximum at 0.5 phr, which actually corresponds to the minimum of MAH content in the gel phase. However, increasing the MAH content in the reactive mixture to 1.5 phr, most of the resulting MAH now lies in the gel phase and the grafting percentage goes through a minimum. At higher MAH concentrations, the MAH content in the gel phase diminishes and the non-reacted MAH content (in the aqueous phase) increases. At the highest MAH content, the percentage of MAH in the organic and gel phases is similar, but the rubber obtained in the extrusion process presents degradation.

One of the objectives of this work is to find the optimum amount of MAH in the grafting reaction to achieve the required mechanical and impact properties of the resulting SBRg-PET blends. *Figure 2* presents results of the mechanical and impact strength

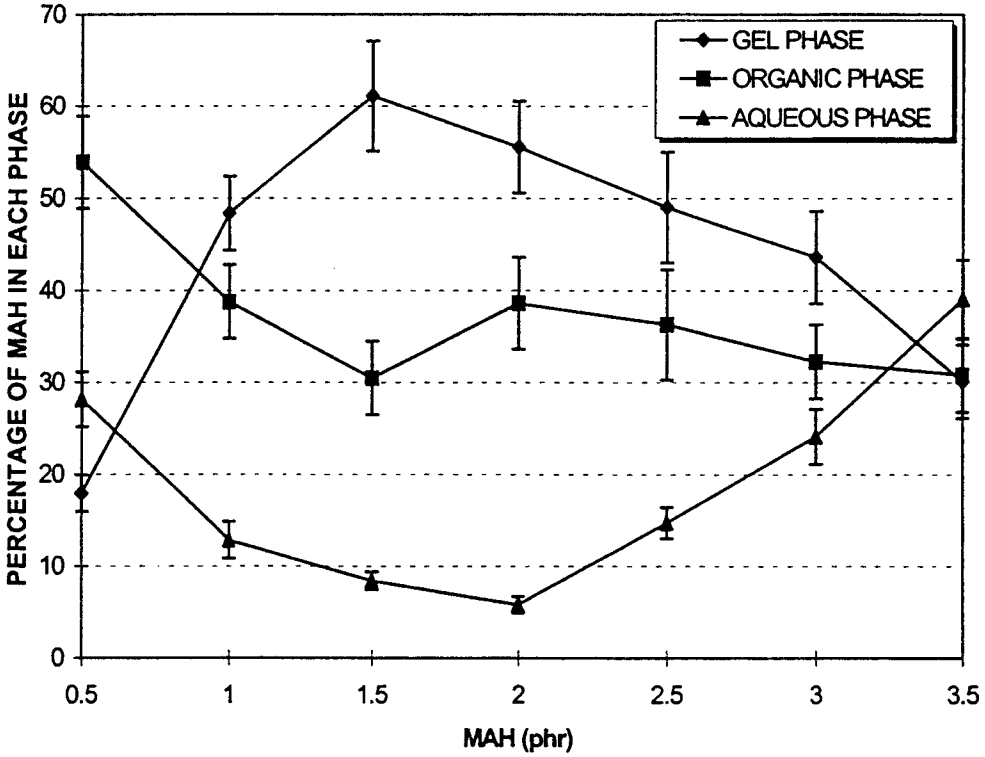

Fig. 1. Reacted MAH percentage present in each phase as a function of initial MAH concentration. T = 160°C, grafting speed = 70 rpm, BPO/MAH = 3%.

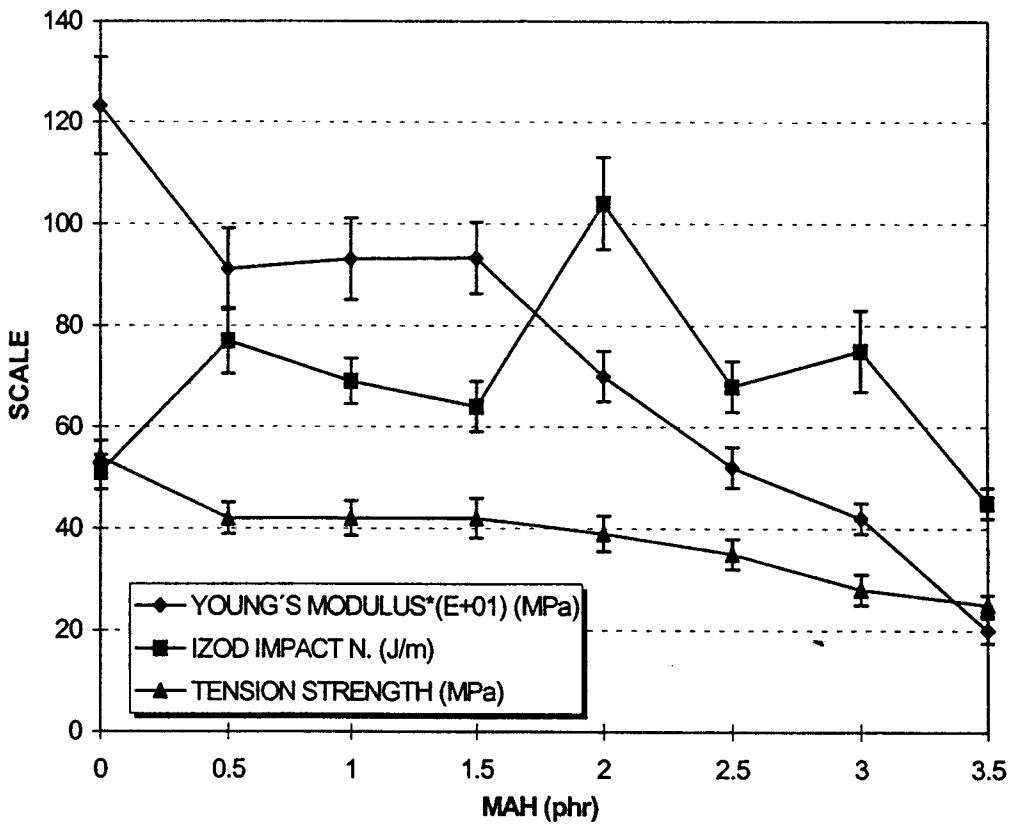

Fig. 2. Mechanical and impact properties of the PET-SBRg blend as a function of initial MAH concentration in the grafting reaction. The SBRg content is 10 phr.

Table 1. Results of the Grafting Reaction.

Sample	Screw Speed	MAH in Organic Phase	MAH in Aqueous Phase	MAH in Gel Phase	Grafting Degree	MAH Reacted/ BPO Added
% BPO/MAH	RPM	%	%	%	%	Mole
0	30	42.90	7.96	49.13	0.6754	—
3	30	41.98	8.58	49.43	0.6609	34.55
7	30	47.16	10.28	42.54	0.7424	16.64
10	30	37.69	7.04	55.26	0.5934	9.308
0	70	37.99	8.58	53.42	0.5980	—
3	70	38.61	5.81	55.57	0.6078	31.78
7	70	47.16	5.54	47.29	0.7424	16.64
10	70	44.12	4.59	51.27	0.6946	10.89
0	100	43.51	7.66	48.82	0.6849	—
3	100	51.78	8.26	39.94	0.8152	42.62
7	100	41.65	6.15	52.19	0.6557	14.70
10	100	46.27	6.12	47.6	0.7284	11.42

evaluations when the SBRg concentration in the blend is 10 phr. Mechanical properties present a continuous decrease for MAH concentrations in the grafting reaction higher than 1.5 phr. On the other hand, the resulting blend presents a remarkable maximum in the impact strength when 2 phr of MAH is used in the grafting reaction. It is noteworthy that the maximum in the impact strength of the blend is obtained with the SBR which does not possess the largest concentration of grafted groups. As shown in *Fig. 1*, the largest grafting degree is obtained with 0.5 phr of MAH. This result is in agreement with data from similar blends obtained elsewhere (39). Mechanical properties, however, have larger values with higher grafted MAH content in the rubber phase.

Similarly, the optimum BPO concentration is estimated by measuring the percentage of MAH present in each phase, but considering now different BPO concentrations in the reacting mixture. As mentioned, the reaction can be carried out without peroxide, since the free radicals may be generated by the thermomechanical work in the extrusion process. BPO concentrations range from zero to ten percent with respect to the MAH amount. To evaluate the effect of the thermomechanical work on the grafting reaction, three extrusion speeds are used (30, 70 and 100 rpm). The resulting grafted double bonds percentage is calculated from the number of moles of MAH reacted with respect to the total MAH added. Considering 30 wt% of styrene groups in SBR, the MAH reacted percentage is calculated per mole of butadiene, and also per mole of BPO. *Table 1* shows the MAH amounts that are present in each phase. Last column presents the MAH-reacted moles per mole of BPO as a function of initial BPO concentration. Observation of a given BPO/MAH ratio indicates that the amount of reacted MAH is similar for two extrusion speeds (30 and 70 rpm), which indicates that at these rotational speeds, the ratio of MAH reacted moles per BPO mole is not a function of the extrusion speed. In the 6th column, the double bond percentage of butadiene grafted with MAH is shown, assuming that one molecule of MAH reacts with a single double bond. The grafting percentage lies approximately between 0.6 and 0.8%. According to these data, the effect of BPO concentration and screw speed on the efficiency of the grafting reaction is small. However, results from mechanical tests may offer another perspective.

Table 2 presents mechanical and impact tests results of PET-SBRg blends, using SBRg (10 phr) produced with various BPO concentrations at different screw speeds. The elastic modulus and tension strength remain practically invariant with respect to screw speed and peroxide content in the mixture. Izod impact results show a maximum at a screw speed of 70 rpm with a 3% of BPO content with respect to the weight of MAH added. The highest screw speed (100 rpm) is likely to cause significant shear degradation of the PET matrix, and this partly explains the drop in impact properties observed in the blend with 10% BPO/MAH content. According to these data, BPO content is important with regard to the magnitude of the impact strength, and thus the combined effect of shear degradation due to high speed and BPO content may offer an explanation of these results.

Impact strength in PET-SBR blends is related to the adhesion between the rubber particle and the PET matrix (40). Different degrees of adhesion between particles and matrix were determined by contact angle measurements on samples prepared following different processing conditions. According to these measurements, for example, the grafted rubber particle with MAH and 3% BPO, processed at 70 rpm, presents better adhesion than that processed at 30 rpm with 7% BPO.

SBR Concentration in the Blend

Once the processing conditions and optimum reactants concentration (MAH, BPO) for the grafting reaction are determined, mechanical and impact properties of PET-SBRg blends prepared with various grafted rubber concentrations (from 3 to 50 phr) are measured, to find the required rubber concentration in the blend for specific applications.

Table 2. Impact and Mechanical Properties of the PET-SBRg Blend for Several Extrusion Speeds for Grafting and BPO/MAH Ratios. SBRg Content in the Blend is 10 phr.

Sample	Screw Speed	Young's Modulus	Tension Strength	Izod Impact Notched
% BPO/MAH	rpm	MPa	MPa	J/m
0	30	651	39.27	82
3	30	676	38.28	64
7	30	658	37.24	80
10	30	639	39.52	69
0	70	650	40.00	41
3	70	683	40.77	103
7	70	659	38.55	67
10	70	630	39.16	77
0	100	651	38.82	64
3	100	647	39.08	71
7	100	641	38.53	80
10	100	530	40.36	54

Figure 3 shows the mechanical and impact properties (elastic modulus, tension strength and Izod impact strength) of the PET-SBRg blends as functions of grafted rubber concentration. The grafting reaction was carried out with 2 phr MAH, 3% of BPO/MAH at 70 rpm. Both the modulus and tension strength decrease as the rubber content increases. This result is expected, since the dispersed phase (rubber) creates stress concentrations and force the material to yield at small strain values. Moreover, as the decrement in the elastic modulus and tension strength is monotonic, it is likely that a good dispersion of rubber particles in the matrix is obtained. Observe that the Izod impact resistance presents a maximum at 15 phr of rubber.

Comparing these results with those obtained using SBR with no grafting, presented in *Fig. 4*, the blend properties show an initial decrease all rubber concentrations, not only in the mechanical but also in the impact properties, due to lack of compatibility (27).

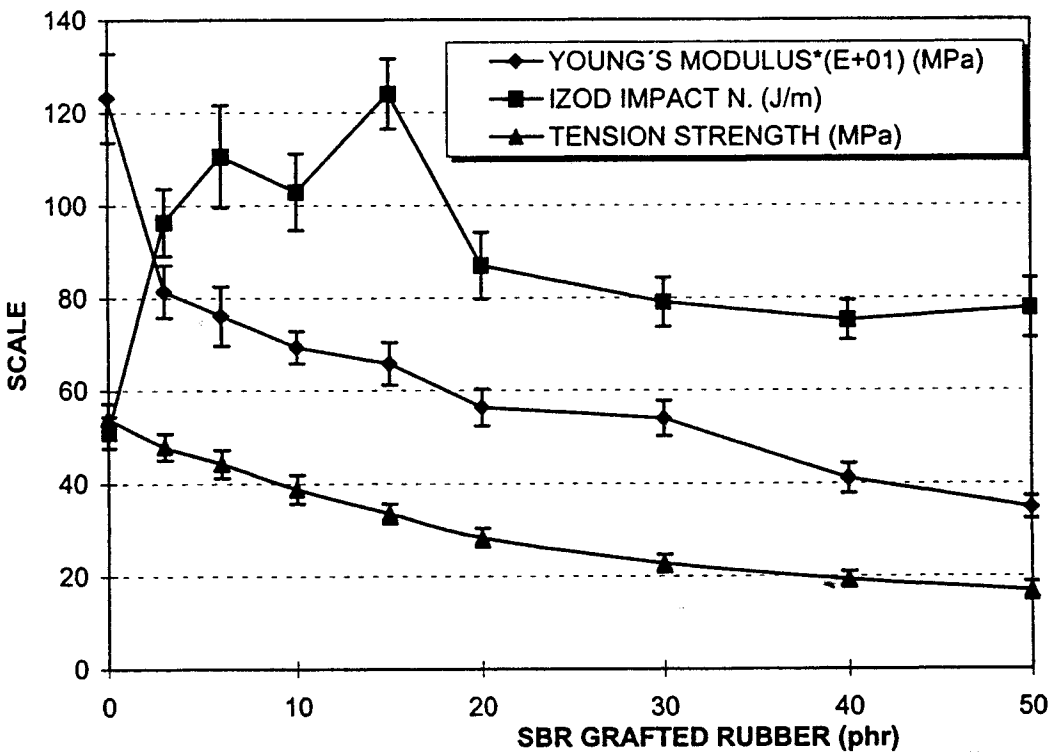

Fig. 3. Impact resistance and mechanical properties of the PET-SBRg blend as functions of SBRg content. Blending speed = 50 rpm, injection speed = 85 mm/s, grafting speed = 70 rpm.

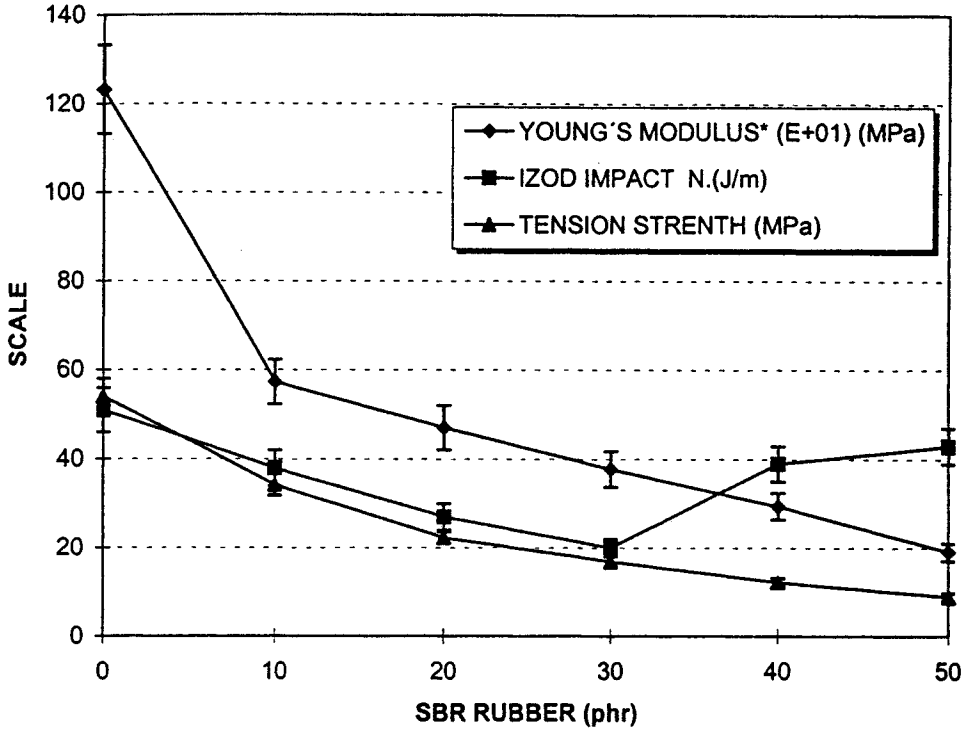

Fig. 4. Impact resistance and mechanical properties of the PET-SBR blend as functions of the SBR content.

Particle Diameter and Interparticle Distances of the Dispersed Phase

Impact properties of the PET-SBRg blends prepared at different extruder speeds (10 to 200 rpm) depend strongly on the microstructure of the blend, i.e., particle sizes and interparticle distances of the dispersed rubber phase (41). Processing conditions are important factors to control microstructure, as shown in *Fig. 5*, where the variation of particle size and interparticle distance are plotted with the screw rotational speed. In the low speed range, as the rotational speed increases, a pronounced decrease in the interparticle distance is observed. The particle diameter remains practically constant up to 40–50 rpm, where a substantial drop in particle size occurs. Thereafter, for larger speeds, particle size remains approximately constant. Simultaneously, the interparticle distance curve changes slope at 40–50 rpm to a more gradual decrease for larger speeds. A small change in the curves is observed between 150 to 175 rpm.

In *Fig. 6*, the impact resistance, particle diameters and distances among particles are plotted as functions of the extrusion speed. Notice that between 40 rpm (corresponding to an average particle diameter of 19.6×10^{-6}m) and 50 rpm (corresponding to a particle diameter of 6.72×10^{-6}m) a remarkable increase in the impact resistance is observed. A second diameter change, although less significant, is observed between 150 rpm (average particle diameter of 5.87×10^{-6}m) and 175 rpm (particle diameter of 4.1×10^{-6}m). The interparticle distance does not present abrupt changes, but a gradual slope change around 50 rpm, which coincides with the maximum in the impact strength of the blend. Hence, interparticle distances as well as the particle diameter govern the performance of the impact strength for a given rubber content.

The experimental results presented above are in qualitative accord with predictions of the model by Wu (41), which points out that in systems with dispersed rubber particles, the impact strength increases substantially when the interparticle distance among particles is smaller than a critical value, even when chemical bonding is present. The critical interparticle distance is thus a material property of the matrix. Wu has shown experimental data of nylon-rubber blends illustrating a sharp tough-brittle transition occurring at a specific interparticle distance, independent of the rubber volume fraction.

This model proposes that a maximum in the impact strength is determined by a critical particle diameter, which itself is a function of the interparticle distance, according to:

$$dc = Tc\,((\pi/(6\,\phi r))^{1/3} - 1)^{-1} \qquad (3)$$

By definition, the surface to surface interparticle distance Tc is a material property of the matrix, independent on the critical diameter dc and also independent on ϕr (rubber volume fraction). For a given rubber volume fraction, predicted values of the critical diameter are obtained from *Eq 3* using experimental values of Tc.

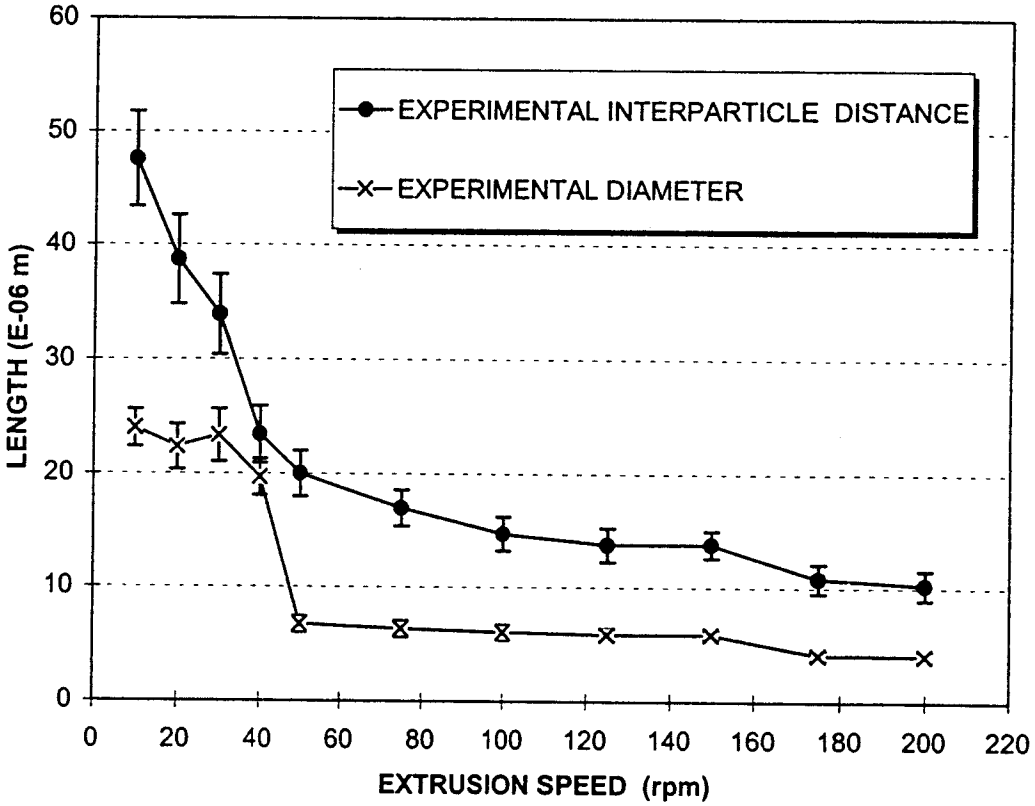

Fig. 5. Particle diameter and interparticle distances in the PET-SBRg blend with 15 phr rubber content as functions of the extrusion speed.

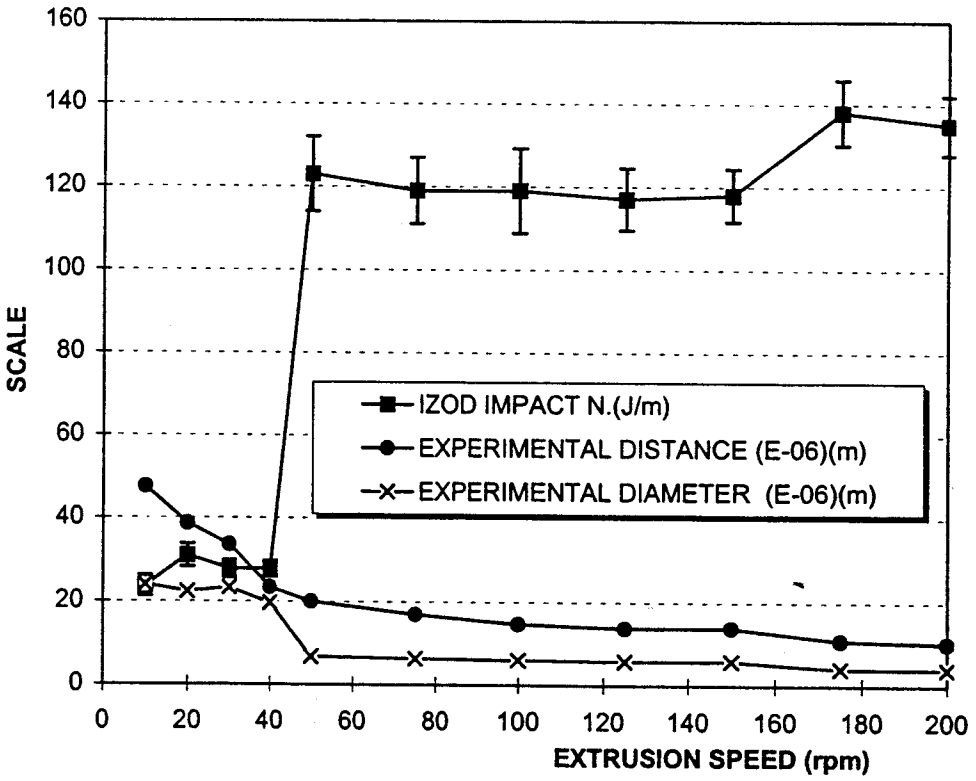

Fig. 6. Impact resistance, particle diameter and interparticle distances in the PET-SBRg blend with 15 phr rubber content as functions of the extrusion speed.

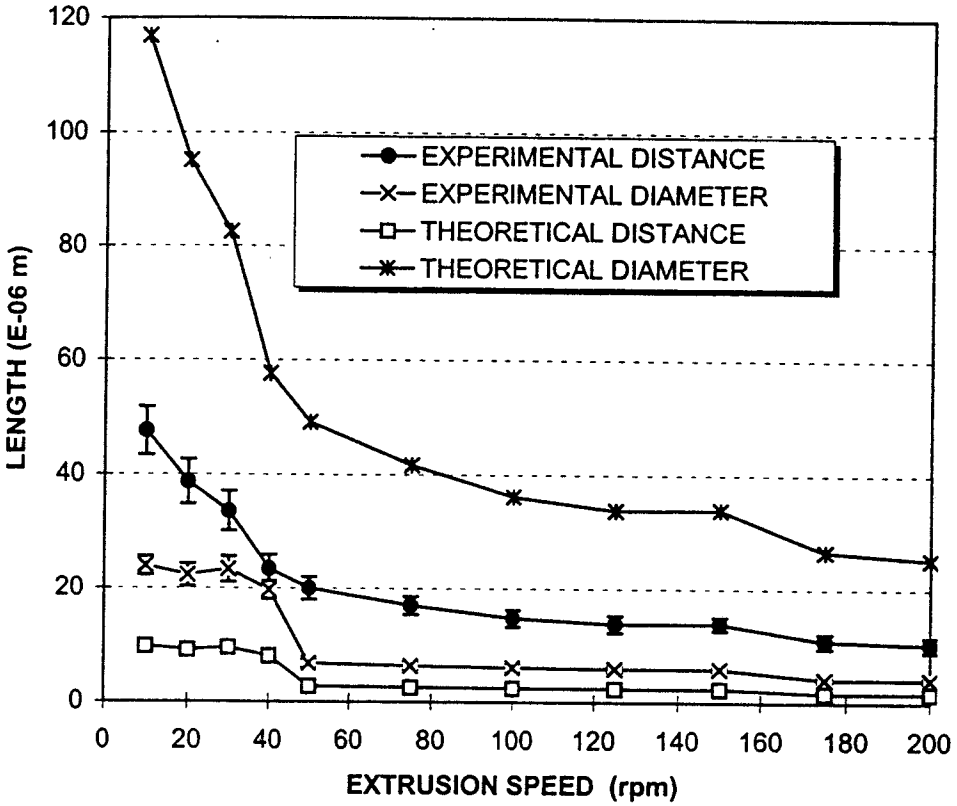

Fig. 7. Experimental data and theoretical predictions from Eq 3 of the particle diameter and interparticle distances in the PET-SBRg blend, with 15 phr rubber content, as functions of the extrusion speed.

Results of the PET-SBRg blends are plotted in *Fig. 7*, which illustrates substantial discrepancies between the experiment and the model predictions.

Wu's model considers a cubic unitary cell with inclusions of spherical rubber particles placed at the cell corners. Since the rubber volume fraction is given by the sphere volume divided by the cell total volume, *Eq 3* may be obtained straightforwardly. Clearly, in *Fig. 7*, discrepancies between predictions and data are observed in the vertical direction. In fact, in a cubic lattice the particles are located in such a way to ensure the symmetry of the primitive cell. To preserve the symmetry of a given cell formed by a number of primitive cells, it is necessary to keep a geometric progression of the number of primitive cells. This is, a given symmetric cell would be formed by 1, 8, 27, ... primitive cells, each one containing one particle. However, if asymmetric arrangements of particles are allowed, it is possible that a primitive cell would contain more than one rubber particle and the ensemble would be asymmetric in this case. The asymmetry does not change the basic qualitative predictions of the model. Instead, only shifts the curve vertically. A given number of 15 particles, for instance, is only a representative degree of asymmetry. Performing simple calculations, *Eq 3* is modified to:

$$dc = Tc\,((N\pi/(6\,\phi\,r))^{1/3} - 1)^{-1} \qquad (4)$$

where N is the number of particles in the arrangement. Besides, Wu (41) has proposed an alternative model (particle concentration model) in which the tough-brittle transition is assumed to occur when the number of particles per unit volume in the blend reaches a critical value. *Eq 4*, therefore, combines both models, the particle concentration model and the interparticle distance model.

In *Fig. 8*, calculations applying *Eq 4* are shown with a number of particles N equal to 15. Notice that the theoretical values agree now with the experimental data within a specific range, reflecting the behavior of the diameter and interparticle distance with extrusion speed quite well for speeds higher than 50 rpm.

Finally, *Fig. 9* shows results of the impact strength and mechanical properties of the blend processed at different screw speeds. The Young's modulus and tension strength do not present significant variations with screw speed. Therefore, although these properties depend on the rubber volume fraction of the blend, they are not direct functions of the particle diameter neither of interparticle distances. This is in contrast to the impact tests results, which present an outstanding increase in the impact strength for extrusion speeds larger than 40 rpm, related directly to particle size and interparticle distances.

CONCLUDING REMARKS

Remarkable increases in the impact strength of SBRg-PET blends are obtained at critical values of rubber particle size and interparticle distance. Optimum

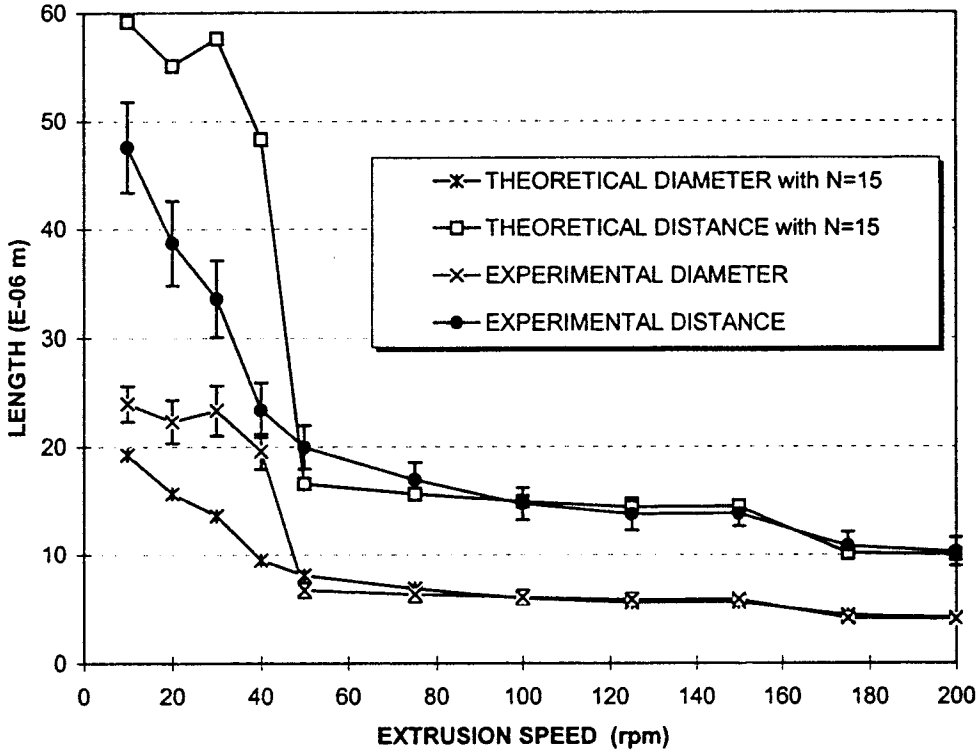

Fig. 8. Experimental data and theoretical predictions from Eq 4 of the particle diameter and interparticle distances in the PET-SBRg blend, with 15 phr rubber content, as functions of the extrusion speed.

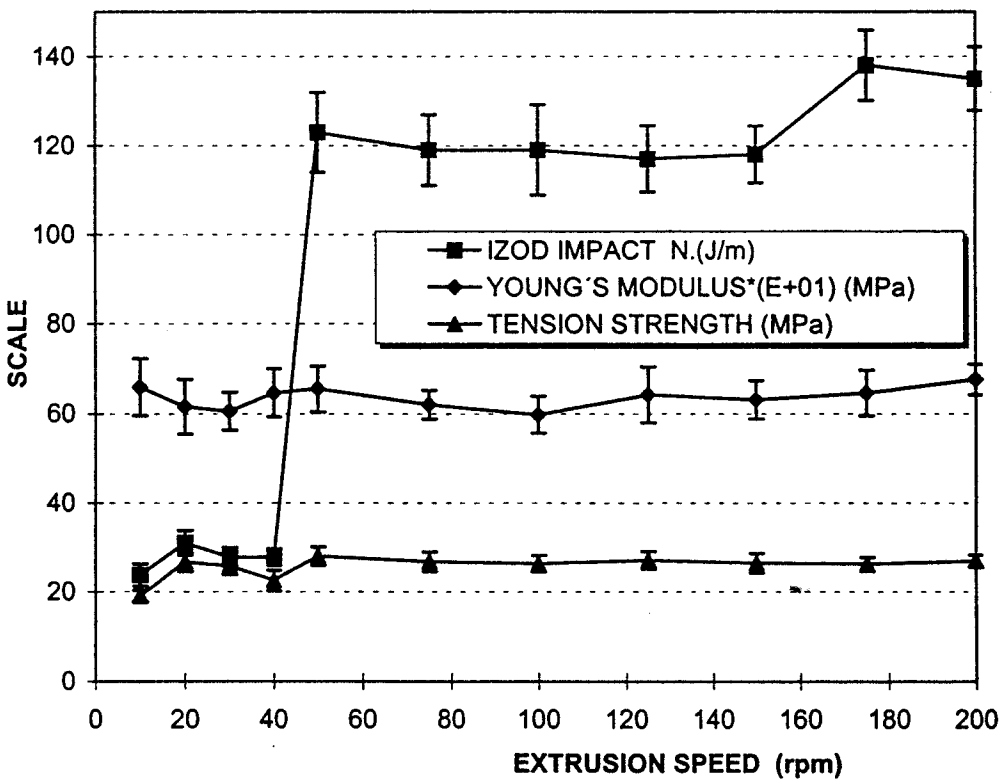

Fig. 9. Mechanical properties and Izod-notched impact results of the PET-SBRg blend with 15 phr rubber content as functions of the extrusion speed.

impact resistance of the blends may be obtained when the MAH concentration in the grafting reaction is 2 phr with a 3 wt% BPO/MAH ratio at 70 rpm. The resulting percentage of grafting in the modified SBR lies between 0.6 and 0.8%. A maximum in the impact strength of the PET-SBRg blends is observed when the modified rubber concentration in the blend is 15 phr. At this concentration, the impact resistance increases approximately 2.5 times with respect to that of pure PET. This increase is governed by a given particle diameter and interparticle distance of the dispersed rubber phase.

Young's modulus and tension strength of the PET-SBRg blend are not functions of the particle diameter neither of the interparticle distance. They depend solely on the rubber concentration in the blend. The model by Wu, which states that the condition for the improvement of the impact strength in a system with dispersed rubber particles is that the surface to surface interparticle distance must be smaller than a critical value, which is a material property of the matrix independent of particle size and rubber volume fraction, does not predict adequately the experimental data. Modifications made on the model to increase the concentration of rubber particles contained in the base cell (rubber volume fraction) allowing an asymmetric layout of particles, yield better predictions of the experimental results.

ACKNOWLEDGMENTS

The authors acknowledge the collaboration of J. Guzmán, A. Maciel, E. Sánchez, F. Martínez, J. Guerra and A. Caballero for the microphotographs, mechanical tests, extruder work, injection molding work, chemical titrations and photografic work, respectively.

REFERENCES

1. F. O. Eduard, B. S. Olga, N. R. Serge, and V. S. Serge, *Polym. Adv. Tech.*, **6**, 1 (1993).
2. H. Munstedt, *Polym. Eng. Sci.*, **21**, 259 (1981).
3. S. Wu, *J. Appl. Polym. Sci.*, **21**, 699 (1983).
4. S. Cimmino, L. D'Oracio, and R. Greco, *Polym. Eng. Sci.*, **24**, 48 (1984).
5. R. Namita and K. B. Anil, *J. Appl. Polym. Sci.*, **38**, 1091 (1989).
6. W. E. Baker and A. M. Catani, *Polym. Eng. Sci.*, **24**, 1348 (1984).
7. J. Crevecoeur, L. Nelissen, and M. van der Sanden, *Polymer*, **36**, 753 (1995).
8. J. K. Kallitsis and N. K. Kalfoglou, *Eur. Polym. J.*, **23**, 117 (1987).
9. J. C. Golba and T. George, *Plastics Engineering*, March 1987, p. 57.
10. B. Puransky, I. Fortelny, and J. Kovar, *Plastics, Rubber and Composites Processing and Applications*, **15** (1), 31 (1991).
11. D. J. Hourston, S. Lane, and H. Zhang, *Polymer*, **32** (6), 1140 (1991).
12. L. A. Utracki, A. M. Catani, and G. L. Bata, *J. Appl. Polym. Sci.*, **27**,1913 (1982).
13. J. W. Song and A. S. Abhiraman, *J. Appl Polym. Sci.*, **27**, 2369 (1982).
14. M. R. Kamal, M. A. Sahto, and L. A. Utracki, *Polym. Eng. Sci.*, **23**, 637 (1983).
15. M. R. Kamal, M. A. Sahto, and L. A. Utracki, *Polym. Eng. Sci.*, **22**, 1127 (1982).
16. L. Z. Pillon and L. A. Utracki, *Polym. Eng. Sci.*, **24**, 1300 (1984).
17. L. Z. Pillon and L. A. Utracki, *Polym. Eng. Sci.*, **27**, 562 (1987).
18. A. Rudin, D. A. Loucks, and J. M. Gulpucasser, *Polym. Eng. Sci.*, **20**, 741 (1980).
19. P. Bataille, S. Boisse, and H. Schreiber, *Polym. Eng. Sci.*, **27**, 622 (1987).
20. L. Mascia and F. Bellahdeb, *Adv. Polym. Tech.*, **13** (2), 99 (1994).
21. K. K. Nikos, S. S. Dimitrios, and D. S. Dionissia, *Polymer*, **35** (17), 3624 (1994).
22. D. F. Nathan and C. J. Ming-Cheng, *J. Appl. Polym. Sci.*, **30**, 2105 (1985).
23. P. M. Subramanian, *Polym. Eng. Sci.*, **27**, 1574 (1987).
24. M. E. Calahorra, J. I. Eguizabal, M. Cotazar, and M. Guzman, *Polym. Communications*, **28**, 39 (1987).
25. M. Cotazar, J. Eguiazabal, and J. Iruin, *Eur. Polym. J.*, **30** (8), 901 (1994).
26. N. K. Kalfoglou and D. S. Skafidas, *Eur. Polym. J.*, **30** (8), 933 (1994).
27. N. Adramova, *Polymer*, **36** (4), 801 (1995).
28. L. Quintanilla, M. Alonso, J. Rodríguez, and M. Pastor, *J. Appl. Polym. Sci.*, **59**, 769 (1996).
29. T. Toda, H. Yoshida, and K. Fukunishi, *Polymer*, **36** (4), 669 (1995).
30. Tercel resin T-97M, *Technical bulletin*, Celanece Mexicana S. A.
31. Solprene 416, *Certificate of quality A-01065*, Industrias Negromex, S. A.
32. J. Sheng, X. Log Lu, and K. De Yao, *J. Macromol. Sci-Chem.*, **27** (2), 167 (1990).
33. N. G. Gaylord, R. Metha, V. Kumar, and M. Tazi, *J. Appl. Polym. Sci.*, **38**, 359 (1989).
34. D. F. Lawson *et al.*, *J. Appl. Polym. Sci.*, **39**, 2331 (1990).
35. Y. Minoura, M. Veda, S. Misunuina, and M. Oba, *J. Appl. Polym. Sci.*, **13**, 1625 (1969).
36. N. Gaylord and M. Metha, *J. Appl. Polym. Sci.*, **20**, 481 (1982).
37. A. J. Muller, J. L. Feijoo, M. E. Alvarez, and A. C. Febles, *Polym. Eng. Sci.*, **27**, 796 (1987).
38. D. M. Fann, S. K. Huang, and J. Y. Lee, *Polym. Eng. Sci.*, **38**, 265 (1998).
39. S. Wu, *Polymer Interface and Adhesion*, pp. 422–24, Marcel Dekker, New York (1982).
40. C. Cimmino, L. D'Orazio, and R. Greco, *Polym. Eng. Sci.*, **24**, 48 (1984).
41. S. Wu, *Polymer*, **26**, 1855 (1985).